marine drugs

MDPI

Article

Lobosteroids A–F: Six New Highly Oxidized Steroids from the Chinese Soft Coral *Lobophytum* sp.

Zi-Yi Xia [1], Man-Man Sun [2], Yang Jin [2], Li-Gong Yao [2], Ming-Zhi Su [2], Lin-Fu Liang [4,*], Hong Wang [1,*] and Yue-Wei Guo [1,2,3,*]

[1] Collaborative Innovation Center of Yangtze River Delta Region Green Pharmaceuticals and College of Pharmaceutical Science, Zhejiang University of Technology, Hangzhou 310014, China; xiaziyi@simm.ac.cn
[2] Shandong Laboratory of Yantai Drug Discovery, Bohai Rim Advanced Research Institute for Drug Discovery, 198 Binhai East Road, High-Tech Zone, Yantai 264117, China; mmsun@baridd.ac.cn (M.-M.S.); yang_jin98@163.com (Y.J.); yaoligong@simm.ac.cn (L.-G.Y.); smz0310@163.com (M.-Z.S.)
[3] School of Medicine, Shanghai University, 99 Shangda Road, Bao Shan District, Shanghai 200444, China
[4] College of Materials Science and Engineering, Central South University of Forestry and Technology, 498 South Shaoshan Road, Changsha 410004, China
* Correspondence: lianglinfu@csuft.edu.cn (L.-F.L.); hongw@zjut.edu.cn (H.W.); ywguo@simm.ac.cn (Y.-W.G.)

Abstract: To explore the steroidal constituents of the soft coral *Lobophytum* sp. at the coast of Xuwen County, Guangdong Province, China, a chemical investigation of the above-mentioned soft coral was carried out. After repeated column chromatography over silica gel, Sephadex LH-20, and reversed-phase HPLC, six new steroids, namely lobosteroids A–F (**1**–**6**), along with four known compounds **7**–**10**, were obtained. Their structures were determined by extensive spectroscopic analysis and comparison with the spectral data reported in the literature. Among them, the absolute configuration of **1** was determined by X-ray diffraction analysis using Cu Kα radiation. These steroids were characterized by either the presence of an α,β-α',β'-unsaturated carbonyl, or an α,β-unsaturated carbonyl moiety in ring A, or the existence of a 5α,8α-epidioxy system in ring B, as well as diverse oxidation of side chains. The antibacterial bioassays showed that all isolated steroids exhibited significant inhibitory activities against the fish pathogenic bacteria *Streptococcus parauberis* FP KSP28, *Phoyobacterium damselae* FP2244, and *Streptococcus parauberis* SPOF3K, with IC_{90} values ranging from 0.1 to 11.0 μM. Meanwhile, compounds **2** and **6**–**10** displayed potent inhibitory effects against the vancomycin-resistant *Enterococcus faecium* bacterium G7 with IC_{90} values ranging from 4.4 to 18.3 μM. Therefore, ten highly oxidized steroids with strong antibacterial activities were isolated from the Chinese soft coral *Lobophytum* sp., which could be developed as new chemotypes of antibacterial drug leads.

Keywords: soft coral; *Lobophytum* sp.; steroids; antibacterial activity

Citation: Xia, Z.-Y.; Sun, M.-M.; Jin, Y.; Yao, L.-G.; Su, M.-Z.; Liang, L.-F.; Wang, H.; Guo, Y.-W. Lobosteroids A–F: Six New Highly Oxidized Steroids from the Chinese Soft Coral *Lobophytum* sp. *Mar. Drugs* **2023**, *21*, 457. https://doi.org/10.3390/md21080457

Academic Editors: Hee Jae Shin and Natalia V. Ivanchina

Received: 26 July 2023
Revised: 17 August 2023
Accepted: 18 August 2023
Published: 19 August 2023

1. Introduction

Unlike terrestrial, the unique and complex marine environment creates rich chemodiversities and biodiversities of secondary metabolites in soft corals [1], such as the bioactive steroids with diverse structural features [2]. Structurally, these soft coral-derived steroids display an array of carbon frameworks, ranging from the usual cholestane [3], ergostane [4], and pregnane-type [5] sterols to the rare secosteroids [6] and highly degraded steroids [7]. Biologically, this group of secondary metabolites exhibit a wide spectrum of bioactivities, including antibacterial [8], anti-inflammatory [9], cytotoxic [10], immunosuppressive [11], and PTP1B inhibitory [6] activities. These properties make steroids attract the continuous attention of chemists and pharmacologists [12].

It is well known that soft corals of the genus *Lobophytum* are one group of the most important marine invertebrates widely distributed in waters. They produce a wealthy biochemical repository of secondary metabolites [13] ranging from terpenoids [14],

steroids [15], prostaglandins [16], and amides [17] to quinones [18]. Among these chemical constituents, steroids are one major group of metabolites that were found in many species of the genus *Lobophytum*, including *Lobophytum sarcophytoides* [9,17], *Lobophytum pauciflorum* [15], *Lobophytum michaelae* [19], *Lobophytum crassum* [20,21], *Lobophytum lobophytum* [22], *Lobophytum compactum* [23], *Lobophytum patulum* [24], and *Lobophytum* spp. [10,25–27]. Notably, these metabolites display various biological activities, such as anticancer [10,15,25], anti-inflammatory [9,17,19], and 5α-reductase inhibitory [28] activities.

As part of our ongoing research aimed at discovering bioactive substances from marine invertebrates in China [29], we recently collected *Lobophytum* sp. at the coast of Xuwen County, Guangdong Province, China. In our recent study, we have reported the isolation and structural elucidation of anti-tumor cembrane diterpenoids from the Hainan specimens of *Lobophytum* sp. [30]. While our current investigation on the Guangdong collection of *Lobophytum* sp. has now resulted in the isolation of six new steroids, lobosteroids A–F (**1**–**6**), together with four known analogs **7**–**10** (Figure 1). The structural difference of six new steroids **1**–**6** is mainly attributed to the different degrees of oxidation in rings A and B of the steroidal nucleus and the variations of functional groups on the side chains. This paper describes the isolation, structural elucidation, and bioactivity of these compounds.

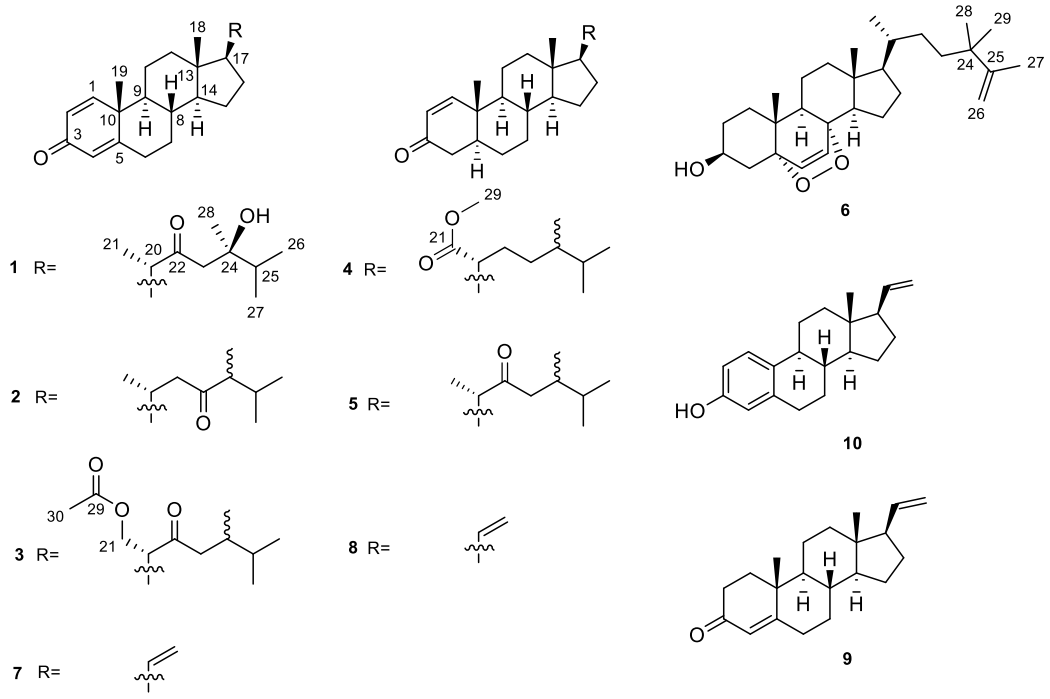

Figure 1. Chemical structures of compounds **1**–**10**.

2. Results and Discussion

The frozen animals were cut into pieces and extracted with acetone exhaustively. The Et_2O-soluble portion of the acetone extract was repeatedly column chromatographed over silica gel, Sephadex LH-20, and reversed-phase HPLC to yield ten pure steroids **1**–**10** (Figure 1). Four known steroids were readily identified as pregna-1,4,20-trien-3-one (**7**) [31], pregna-1,20-dien-3-one (**8**) [32], pregna-4,20-dien-3-one (**9**) [33], and 19-norpregna-1,3,5(10),20-tetraen-3-ol (**10**) [34], respectively, by comparison of their NMR data and optical rotation $[\alpha]_D$ values with those reported in the literature.

Compound **1**, colorless crystals, had the molecular formula of $C_{28}H_{42}O_3$ as established by HRESIMS (Figure S7) from the protonated molecular ion peak observed at m/z 427.3210 $[M + H]^+$ (calcd. 427.3207), implying eight degrees of unsaturation. Extensive analysis of ^{13}C NMR and DEPT spectra of **1** (Table 1, Figure S2) disclosed the presence of 28 carbons, consisting of six methyls, seven sp^3 methylenes, six sp^3 methines,

three sp^3 quaternary carbons (including one oxygenated at δ_C 74.0), three sp^2 methines (δ_C 124.1, 127.7, and 155.8), and three sp^2 quaternary carbons (including one olefinic at δ_C 169.1 and two carbonylic at δ_C 186.5 and 217.6). Thus, compound **1** still required a four-ring system to satisfy the remaining four degrees of unsaturation. Considering the co-isolated known metabolites, compound **1** was likely a steroid whose basic nucleus was a fused four-ring carbon framework. Overall, the gross ^{1}H and ^{13}C spectral data of **1** (Tables 1 and 2, Figures S1 and S2) were reminiscent of 24-methylenecholesta-1,4,24(28)-trien-3-one, a sterol previously reported from the soft coral *Dendronephthya studeri* [35]. Careful comparison of their NMR data revealed they possessed the same steroidal nucleus possessing an α,β-α',β'-unsaturated carbonyl moiety, which was straightforward from NMR signals at δ_H 7.05 (d, J = 10.2 Hz, H-1), 6.23 (dd, J = 10.2, 2.0 Hz, H-2), 6.07 (br s, H-4), and δ_C 155.8 (d, C-1), 127.7 (d, C-2), 186.5 (s, C-3), 124.1 (d, C-4), 169.1 (s, C-5) (Figure S3). The establishment of ring A was further confirmed by the key HMBC correlations from H_3-19 (δ_H 1.10) to C-1 (δ_C 155.8), C-5 (δ_C 169.1), C-9 (δ_C 52.3), and C-10 (δ_C 43.6), from H-1 (δ_H 7.05) to C-3 (δ_C 186.5) and C-5, from H-2 (δ_H 6.23) to C-4 (δ_C 124.1) and C-10, and from H-4 (δ_H 6.07) to C-6 (δ_C 33.0) and C-10 (Figures 2 and S4). However, they differed in the structures of their side chains. First, the methylene C-22 in 24-methylenecholesta-1,4,24(28)-trien-3-one was oxidized into a ketone in **1**, which was characterized by the remarkably down-field chemical shift of δ_C 217.6 (s, C-22). Secondly, the terminal double bond $\Delta^{24(28)}$ in 24-methylenecholesta-1,4,24(28)-trien-3-one was reduced in **1**, accompanied with the hydroxylation at C-24, which was indicated by the NMR signals at δ_H 1.12 (s, H_3-28) and δ_C 23.0 (q, C-28), 74.0 (s, C-24). Furthermore, the structure of the side chain in **1** was verified clearly by the HMBC correlations from H_3-21 (δ_H 1.10) to C-17 (δ_C 52.0), C-20 (δ_C 50.9) and C-22 (δ_C 217.6), from H_2-23 (δ_H 2.53, 2.66) to C-22 and C-24 (δ_C 74.0), and from H_3-28 to C-23 (δ_C 48.2), C-24 and C-25 (δ_C 37.4) (Figures 2 and S4). Herein, the planar structure of **1** was determined as depicted in Figure 1. The observed NOE correlations regarding the chiral centers C-8, C-9, C-10, C-13, C-14, C-17, and C-20, and the double bonds Δ^1 and Δ^4 of **1** (Figures 2 and S6) were similar to those of 24-methylenecholesta-1,4,24(28)-trien-3-one, suggesting they shared the same relative configurations for these stereocenters and double bonds. However, there were insufficient NOE correlations to assign the relative configuration of C-24. Luckily, suitable single crystals of **1** in MeOH were obtained. The X-ray crystallographic analysis using Cu Kα radiation (λ = 1.54178 Å) firmly disclosed the absolute configuration of **1** was 8*S*,9*S*,10*R*,13*S*,14*S*,17*R*,20*S*,24*R* (Flack parameter: 0.09 (8), Figure 3).

Table 1. ^{13}C NMR data of compounds **1**–**6** in $CDCl_3$.

No.	1 [a]	2 [b]	3 [a]	4 [a]	5 [a]	6 [c]
	δ_C (Mult.)	δ_C (Mult.)	δ_C (Mult.)	δ_C (Mult.)	δ_C (Mult.)	δC (Mult.)
1	155.8 (d)	156.2 (d)	155.7 (d)	158.7 (d)	158.6 (d)	34.8 (t)
2	127.7 (d)	127.6 (d)	127.8 (d)	127.5 (d)	127.6 (d)	30.3 (t)
3	186.5 (s)	186.6 (s)	186.5 (s)	200.4 (s)	200.4 (s)	66.6 (d)
4	124.1 (d)	123.9 (d)	124.1 (d)	41.1 (t)	41.1 (t)	37.1 (d)
5	169.1 (s)	169.5 (s)	169.0 (s)	44.4 (d)	44.4 (d)	82.3 (s)
6	33.0 (t)	33.0 (t)	32.9 (t)	27.7 (t)	27.7 (t)	135.6 (d)
7	33.7 (t)	33.8 (t)	33.6 (t)	32.1 (t)	31.4 (t)	130.9 (d)
8	35.6 (d)	35.6 (d)	35.6 (d)	35.8 (d)	35.8 (d)	79.6 (s)
9	52.3 (d)	52.4 (d)	52.2 (d)	50.1 (d)	49.9 (d)	51.2 (d)
10	43.6 (s)	43.8 (s)	43.6 (s)	39.1 (s)	39.1 (s)	37.1 (s)
11	22.9 (t)	24.5 (t)	22.8 (t)	30.1 (t)	21.3 (t)	23.5 (t)
12	39.5 (t)	39.5 (t)	38.8 (t)	37.5 (t)	39.8 (t)	39.5 (t)
13	43.1 (s)	42.9 (s)	43.0 (s)	42.4 (s)	43.1 (s)	44.8 (s)
14	54.9 (d)	55.6 (d)	54.6 (d)	55.8 (d)	55.8 (d)	51.7 (d)
15	24.7 (t)	23.0 (t)	24.5 (t)	23.8 (t)	24.5 (t)	20.8 (t)
16	27.5 (t)	28.4 (t)	26.9 (t)	27.3 (t)	27.7 (t)	28.3 (t)
17	52.0 (d)	56.0 (d)	49.6 (d)	52.9 (d)	52.4 (d)	56.2 (d)
18	12.4 (q)	12.2 (q)	12.5 (q)	12.4 (q)	12.6 (q)	12.7 (q)

Table 1. *Cont.*

No.	1 [a]	2 [b]	3 [a]	4 [a]	5 [a]	6 [c]
	δ_C (Mult.)	δ_C (Mult.)	δ_C (Mult.)	δ_C (Mult.)	δ_C (Mult.)	δC (Mult.)
19	18.8 (q)	18.8 (q)	18.8 (q)	13.1 (q)	13.1 (q)	18.3 (q)
20	50.9 (d)	32.0 (d)	53.6 (d)	48.0 (d)	50.0 (d)	35.8 (d)
21	16.4 (q)	20.0 (q)	64.6 (t)	176.9 (s)	16.7 (q)	18.9 (q)
22	217.6 (s)	49.2 (t)	211.8 (s)	29.8 (t)	214.8 (s)	30.4 (t)
23	48.2 (t)	215.0 (s)	49.6 (t)	21.2 (t)	46.8 (t)	37.1 (t)
24	74.0 (s)	53.0 (d)	33.3 (d)	38.7 (d)	33.8 (d)	38.8 (s)
25	37.4 (d)	30.2 (d)	32.1 (d)	31.4 (d)	32.1 (d)	152.3 (s)
26	17.0 (q)	18.8 (q)	18.6 (q)	17.5 (q)	18.3 (q)	109.6 (t)
27	17.9 (q)	21.6 (q)	19.9 (q)	20.6 (q)	20.0 (q)	19.5 (q)
28	23.0 (q)	12.7 (q)	16.2 (q)	15.3 (q)	16.1 (q)	27.3 (q)
29			170.7 (s)	51.2 (q)		27.7 (q)
30			21.0 (q)			

[a] Recorded at 125 MHz. [b] Recorded at 150 MHz. [c] Recorded at 200 MHz.

Table 2. ^{1}H NMR data of compounds **1**–**6** in $CDCl_3$.

No.	1 [a]	2 [b]	3 [a]	4 [a]	5 [a]	6 [c]
	δH Mult. (*J* in Hz)	δH Mult. (*J* in Hz)	δH Mult. (*J* in Hz)	δH Mult. (*J* in Hz)	δH Mult. (*J* in Hz)	δH Mult. (*J* in Hz)
1	7.04 d (10.2)	7.05 d (10.1)	7.03 d (10.1)	7.11 d (10.2)	7.13 d (10.2)	1.70 br d (13.8)
						1.94 dd (13.8, 4.0)
2	6.23 dd (10.2, 2.0)	6.22 dd (10.1, 1.9)	6.23 dd (10.1, 1.9)	5.84 dd (10.2, 1.0)	5.85 d (10.2)	1.54 ovl
						1.84 br d (12.8)
3						3.97 tt (11.2, 5.1)
4	6.07 br [d] s	6.06 br s	6.07 br s	2.21 dd (14.5, 3.6)	2.23 dd (14.9, 3.3)	1.91 ovl
				2.35 dd (17.7, 14.2)	2.36 dd (17.8, 14.2)	2.11 dd (13.7, 5.2)
5				1.90 ovl	1.91 ovl	
6	2.35 br d (13.5)	2.36 br d (13.4)	2.35 br d (13.0)	1.37 m	1.31 ovl	6.24 d (8.5)
	2.45 dd (14.0, 5.2)	2.45 ovl	2.46 dd (13.6, 4.0)	1.42 ovl	1.42 ovl	
7	1.93 m	1.03 ovl	1.06 ovl	0.96 ovl	0.96 m	6.50 d (8.6)
	2.48 dd (12.0, 5.0)	1.94 ovl	1.94 ovl	1.70 ovl	1.71 ovl	
8	1.61 ovl [d]	1.62 ovl	1.61 m	1.45 ovl	1.45 ovl	
9	1.59 ovl	1.04 ovl	1.06 ovl	0.96 ovl	0.99 m	1.49 ovl
11	1.07 m	1.15 ovl	1.66 ovl	0.85 dd (13.1, 6.0)	0.88 m	1.20 ovl
	1.69 ovl	1.61 ovl	1.71 m	1.72 dd (13.3, 3.2)	1.76 dd (13.7, 3.5)	1.50 ovl
12	1.28 td (13.0, 5.0)	1.17 dd (12.5, 6.6)	1.23 ovl	1.07 ovl	1.31 ovl	1.21 ovl
	1.97 dt (13.1, 3.3)	2.04 dt (13.0, 3.3)	1.90 dt (12.6, 3.3)	1.50 ovl	1.97 dt (12.7, 3.4)	1.96 dd (13.3, 3.3)
14	1.04 m	1.00 m	1.01 m	1.08 ovl	1.09 ovl	1.53 ovl
15	1.18 ovl	1.62 ovl	1.20 ovl	1.09 ovl	1.11 ovl	0.89 m
	1.63 td (13.0, 3.5)	1.68 td (11.1, 3.7)	1.64 ovl	1.64 ovl	1.60 ovl	1.64 m
16	1.18 ovl	1.25 m	1.30 m	1.30 ovl	1.32 ovl	1.34 m
	1.73 ovl	1.79 ddd (16.2, 7.0, 3.1)	1.65 ovl	1.90 ovl	1.69 ovl	1.90 ovl
17	1.60 ovl	1.13 m	1.60 ovl	1.65 ovl	1.63 ovl	1.18 ovl
18	0.76 s	0.78 s	0.81 s	0.72 s	0.72 s	0.78 s
19	1.23 s	1.23 s	1.23 s	0.99 s	1.01 s	0.89 s
20	2.48 ovl	2.03 ovl	2.84 td (10.4, 4.4)	2.20 dt (7.5, 3.6)	2.50 dq (10.4. 6.8)	1.32 m
21	1.11 d (7.6)	0.90 d (7.0)	3.96 t (10.7)		1.09 d (6.9)	0.89 d (6.9)
			4.48 dd (10.7, 4.4)			
22		2.20 dd (17.0, 10.0)		1.27 ovl		1.17 ovl
		2.45 dd (17.2, 2.8)		1.40 ovl		1.26 m
23	2.52 d (17.7)		2.22 dd (17.7, 9.1)	1.39 ovl	2.17 dd (16.9, 8.9)	1.17 ovl
	2.66 d (17.7)		2.47 dd (17.5, 3.8)	1.51 ovl	2.45 dd (17.0, 4.3)	1.37 m

Table 2. *Cont.*

No.	1 [a]	2 [b]	3 [a]	4 [a]	5 [a]	6 [c]
	δH Mult. (*J* in Hz)	**δH Mult. (*J* in Hz)**	**δH Mult. (*J* in Hz)**	**δH Mult. (*J* in Hz)**	**δH Mult. (*J* in Hz)**	**δH Mult. (*J* in Hz)**
24		2.29 quin (6.9)	1.94 ovl	1.24 ovl	1.93 ovl	
25	1.75 quin (6.9)	1.92 ovl	1.55 m	1.55 m	1.55 m	
26	0.88 d (6.9)	0.84 d (6.8)	0.83 d (7.1)	0.75 d (6.9)	0.82 d (6.8)	4.65 br s 4.72 br s
27	0.93 d (6.8)	0.90 d (7.0)	0.87 d (6.8)	0.84 d (6.8)	0.87 d (6.8)	1.67 s
28	1.12 s	0.98 d (6.9)	0.81 d (7.6)	0.76 d (6.9)	0.81 d (6.8)	1.00 s
29				3.65 s		1.00 s
30			2.00 s			
OH	4.09 s					

[a] Recorded at 600 MHz. [b] Recorded at 800 MHz. [c] Recorded at 400 MHz. [d] ovl: overlapped, br: broad.

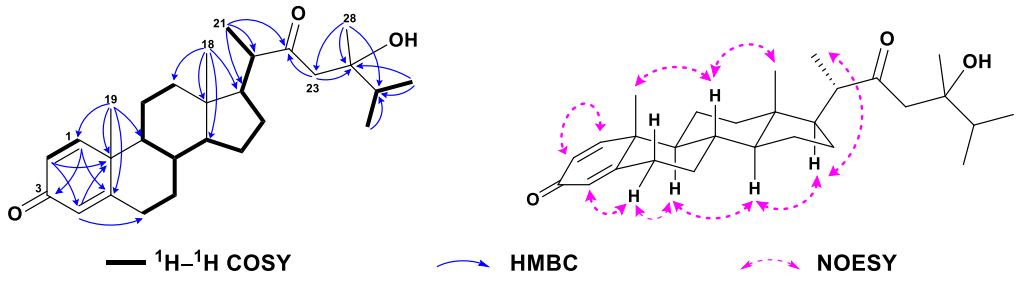

Figure 2. ^{1}H–^{1}H COSY, selected key HMBC and NOE correlations of **1**.

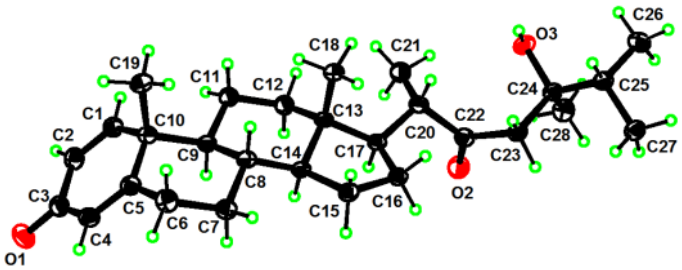

Figure 3. Perspective ORTEP drawing of **1** (displacement ellipsoids are drawn at the 50% probability level).

Compound **2** was obtained as a white amorphous powder and it displayed a protonated molecular ion peak at *m*/*z* 411.3255 ([M + H]$^{+}$; calcd. 411.3258) in the HRESIMS spectrum (Figure S15), consistent with a molecular formula of $C_{28}H_{42}O_2$. Inspection of the NMR data of compound **2** (Tables 1 and 2, Figures S9 and S10) revealed its spectroscopic features were closely similar to those of **1**, suggesting that they possessed the same steroidal nucleus with an *α*,*β*-*α*′,*β*′-unsaturated carbonyl moiety [δ_H 7.05 (d, *J* = 10.1 Hz, H-1), 6.22 (dd, *J* = 10.1, 1.9 Hz, H-2), 6.06 (br s, H-4), and δ_C 156.1 (d, C-1), 127.6 (d, C-2), 186.6 (s, C-3), 123.9 (d, C-4), 169.5 (s, C-5)]. In fact, the differences between **2** and **1** were in the structures of their side chains. The carbonyl group shifted from C-22 in **1** to C-23 (δ_C 215.0) in **2**, and the hydroxyl group attached to C-24 (δ_C 74.0 vs. δ_C 53.0) in **1** was lost in **2**, which was consistent with their 16 mass units difference. The characteristic ^{1}H–^{1}H COSY correlations from H-17 (δ_H 1.13) through H-20 (δ_H 2.04) to H_2-22 (δ_H 2.20, 2.44) and from H_3-28 (δ_H 0.98) through H-24 (δ_H 2.29) and H-25 (δ_H 1.92) to H_3-26 (δ_H 0.84)/H_3-27 (δ_H 0.90), together with the diagnostic HMBC correlations from H_2-22 to C-20 (δ_C 32.0) and C-23, from H_3-28 to C-23, C-24, and C-25 (δ_C 30.2) (Figures 4, S12 and S13), supported the above-mentioned structure of the side chain. The literature surveys revealed that the NMR data of the side chain of **2** were almost identical to those of the synthetic steroid 3*β*-hydroxyergost-5,7-diene-23-one [36], further confirming the

established structure of the side chain. Due to the isomerization of a single isolated chiral center C-24 in a linear chain would not result in significant shifts of ^{1}H or ^{13}C NMR data, the configuration of C-24 was undetermined. Similar NOE correlations as those of **1** were observed in the NOESY spectrum of **2** (Figures 4 and S14), suggesting they had the same relative configurations for the chiral centers of the parent nucleus. Thus, the structure of **2** was depicted as shown in Figure 1.

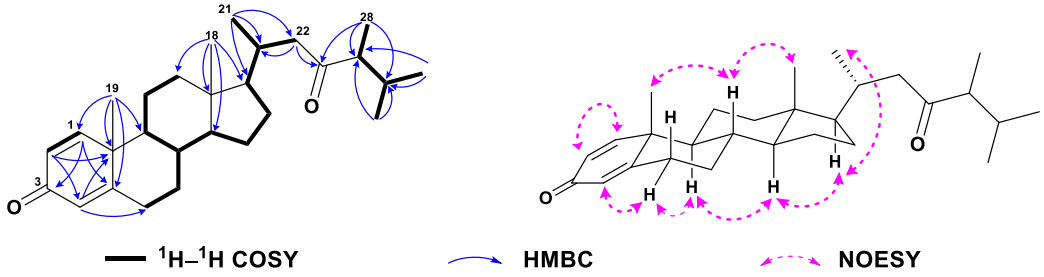

Figure 4. ^{1}H–^{1}H COSY, selected key HMBC and NOE correlations of **2**.

Compound **3**, a white amorphous powder, had the molecular formula of $C_{30}H_{44}O_4$ as established by HRESIMS (Figure S23) from the protonated molecular ion peak observed at m/z 469.3318 $[M + H]^+$ (calcd. 469.3312). Detailed analysis of NMR data of **3** (Tables 1 and 2, Figures S17 and S18) disclosed that **3** and **1** possessed the same steroidal nucleus but differed in the side chain. The presence of an acetyl group in **3** was recognized by the characteristic NMR signals at δ_H 2.00 (s, H_3-30) and δ_C 170.7 (s, C-29), and 21.0 (q, C-30) (Figure S19). The location of the acetyl group at C-21 was straightforward from the significant down-field shifted NMR signals at δ_H 4.48 (dd, J = 10.7, 4.4 Hz, H_a-21), 3.96 (t, J = 10.7 Hz, H_b-21), and δ_C 64.6 (t, C-21), which was further established by the diagnostic HMBC correlations from H_2-21 to C-17 (δ_C 49.5), C-20 (δ_C 53.6), C-22 (δ_C 211.8), and C-29 (δ_C 170.7) (Figures 5 and S20). Moreover, the chemical shift of C-24 (δ_C 38.7) shifted significantly upfield, which indicated that the hydroxyl group attached to C-24 in **1** was lost in **3**. Based on the analysis of the NOE correlations, as depicted in Figures 5 and S22, the structure of **3** was determined, as shown in Figures 1. However, the configuration of C-24 could not be assigned herein.

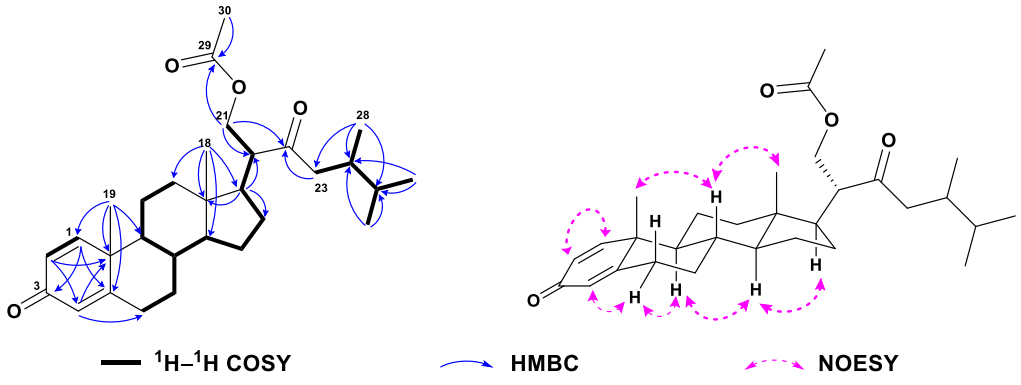

Figure 5. ^{1}H–^{1}H COSY, selected key HMBC and NOE correlations of **3**.

Compound **4** was obtained as a white amorphous powder. Its molecular formula, $C_{29}H_{46}O_3$, was deduced from its protonated molecular ion peak observed at m/z 443.3520 ($[M + H]^+$; calcd. 443.3520) in the HRESIMS spectrum (Figure S31). Careful analysis of its ^{1}H and ^{13}C NMR data (Tables 1 and 2, Figures S25 and S26) revealed the presence of an α,β-unsaturated carbonyl group [δ_H 7.11 (d, J = 10.2 Hz, H-1), 5.84 (dd, J = 10.2, 1.0 Hz, H-2), and δ_C 158.7 (d, C-1), 127.5 (d, C-2), 200.4 (s, C-3)] and a methyl ester functionality [δ_H 3.65 (s, H_3-29) and δ_C 176.9 (s, C-21), 51.2 (s, C-29)] in the molecule. Searching in our

compound library, it was found that the ^{13}C NMR data of C-1–C-21 were nearly identical to those of methyl spongoate, a steroid previously reported from the soft coral *Spongodes* sp. by our group [37], suggesting they had the same steroidal nucleus and a methoxycarbonyl group at C-21 of the side chain. The only difference between them was at the methyl at C-24 in **4**, which was deduced from the ^{1}H–^{1}H COSY correlations from H_3-28 (δ_H 0.76) through H-24 (δ_H 1.24) and H-25 (δ_H 1.55) to H_3-26 (δ_H 0.75)/H_3-27 (δ_H 0.84) as well as the HMBC correlations from H_3-28 to C-23 (δ_C 21.2), C-24 (δ_C 38.7), and C-25 (δ_C 31.4) (Figures 6, S28 and S29). The established structure of the side chain was further verified in agreement with the ^{13}C NMR data of those of (24*S*)-3β-acetoxyergost-5-en-21-oic acid, a secondary metabolite previously reported from the soft coral *Cladiella australis* [38]. Similar NOE correlations as those of methyl spongoate were observed in the ROESY spectrum of **4** (Figures 6 and S30), suggesting they had the same relative configurations for the chiral centers of the parent nucleus. Therefore, compound **4** was established as a 24-methyl derivative of methyl spongoate, as shown in Figure 1, with the configuration of C-24 remaining unknown.

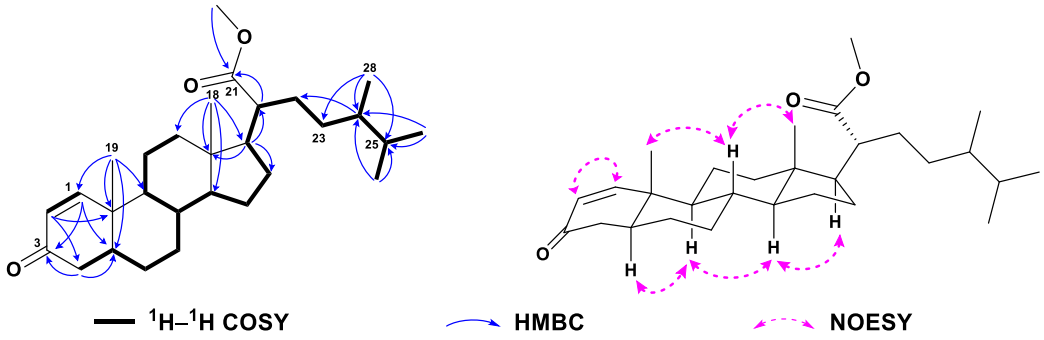

Figure 6. ^{1}H–^{1}H COSY, selected key HMBC and NOE correlations of **4**.

Compound **5** was obtained as a white amorphous powder, and its molecular formula was established as $C_{28}H_{44}O_2$ according to the protonated molecular ion at m/z 413.3411 ([M + H]$^+$; calcd. 413.3414) in the HRESIMS spectrum (Figure S39). A comparison of overall ^{1}H and ^{13}C NMR data (Tables 1 and 2, Figures S33 and S34) revealed that **5** shared the identical steroidal nucleus with **4** but differed at the side chain, where the presence of a ketone at C-22 and the disappearance of a methoxycarbonyl group at C-21 were observed. These differences were evident by the NMR signals at δ_H 1.09 (d, J = 6.9 Hz, H_3-21)/δ_C 16.7 (q, C-21) and δ_C 214.8 (s, C-22) (Figure S35). The ^{1}H–^{1}H COSY correlations from H-17 (δ_H 1.63) through H-20 (δ_H 2.50) to H_3-21 (δ_H 1.08), together with the HMBC correlations from H_3-21 to C-17 (δ_C 52.4), C-20 (δ_C 49.9), and C-22 (δ_C 214.8) and from H-23 (δ_H 2.17) to C-22 and C-24 (δ_C 38.7) (Figures 6, S36 and S37) supported the speculation. Furthermore, the coincident ^{13}C NMR data from C-20 to C-25 and C-28 for **5** and the synthetic steroid 3β-hydroxyergost-5,7-diene-22-one [36] confirmed they shared the same side chain. Based on the analysis of the ROESY correlations, as depicted in Figures 7 and S38, the structure of **5** was determined with the unknown configuration of C-24, as shown in Figure 1.

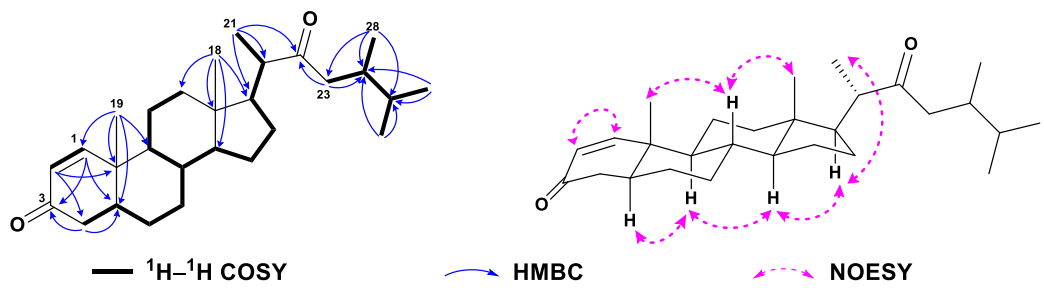

Figure 7. ^{1}H–^{1}H COSY, selected key HMBC and NOE correlations of **5**.

Compound **6** was obtained as a white amorphous powder. Its molecular formula $C_{29}H_{46}O_3$ was determined by the HREIMS ion peak at m/z 424.3325 $[M - H_2O]^+$ (calcd. 424.3336, Figure S47), corresponding to seven degrees of unsaturation. Two vicinal coupled olefinic protons at δ_H 6.24 (d, J = 8.5 Hz, H-6) and 6.50 (d, J = 8.6 Hz, H-7) and an oxygenated methine at δ_H 3.97 (tt, J = 11.2, 5.1 Hz, H-3) were characteristic of a 3β-hydroxy-6-en-5α,8α-epidioxysterol nucleus, which was also recognized by the ^{13}C NMR signals at δ_C 66.6 (d, C-3), 82.3 (s, C-5), 135.6 (d, C-6), 130.9 (d, C-7), and 79.6 (s, C-8) (Figure S43). These spectral data of **6** (Tables 1 and 2, Figures S41 and S42) were reminiscent of yalongsterol A, a sterol previously reported from the soft coral *Sinularia* sp. by our group [11]. Detailed comparison of the full ^{1}H and ^{13}C NMR data of **6** with yalongsterol A, showing great similarity between them, clearly allowed the assignment of 3β-hydroxy-6-en-5α,8α-epidioxy-cholesta nucleus to **6**, which was further justified by the extensive analyses of 2D NMR spectra involving ^{1}H–^{1}H COSY, HSQC, and HMBC (Figures 8 and S43–S45). However, they differed at the side chain. The NMR signals at δ_H 4.72 (br s, H_a-26), 4.65 (br s, H_b-26), 1.67 (s, H_3-27) and δ_C 152.3 (d, C-25), 109.6 (d, C-26), 19.5 (q, C-27) indicated the presence of a terminal double bound with an allylic methyl in the terminal of the side chain of **6**, which was supported by the HMBC correlations from H_2-26 (δ_H 4.65, 4.72) to C-24 (δ_C 38.8), C-25 (δ_C 152.3) and C-27 (δ_C 19.5), H_3-27 (δ_H 1.67) to C-24, C-25 and C-26 (δ_C 109.6) (Figures 8 and S44). Additional HMBC correlations from H_3-28 (δ_H 1.00) to C-23 (δ_C 37.1), C-24, C-25, and C-29 (δ_C 27.7), from H_3-29 (δ_H 1.00) to C-23, C-24, C-25, and C-28 (δ_C 27.3) (Figures 8 and S44) implied the location of germinal methyls at C-24 of the side chain of **6**. With the established structure of the side chain in hand, the structure of **6** was depicted as shown in Figure 1.

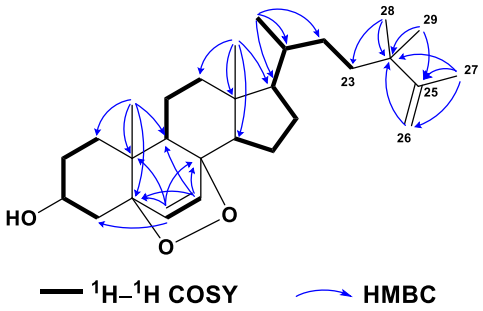

Figure 8. ^{1}H–^{1}H COSY and selected key HMBC correlations of **6**.

In in vitro bioassays, all the isolates were tested for antibacterial, neuroprotective, and anti-inflammatory effects. In the antibacterial bioassays (Table 3), all the steroids exhibited significant antibacterial activities against the fish pathogenic bacteria *Streptococcus parauberis* FP KSP28, *Phoyobacterium damselae* FP2244, and *Streptococcus parauberis* SPOF3K with IC_{90} values ranging from 0.1 to 11.0 μM. As observed in Table 3, the steroids possessing the unsaturated carbonyl moiety in ring A were favored for the inhibition against *Streptococcus parauberis* FP KSP28. Moreover, it seemed that a vinyl-type side chain in the steroid could lead to a small increase in the antibacterial activities against *Phoyobacterium damselae* FP2244 and *Streptococcus parauberis* SPOF3K, as indicated in Table 3. Only compound **7** displayed potent inhibitory activity against the fish pathogenic bacterium *Aeromonas salmonicida* AS42 with an IC_{90} value of 8.8 μM. This might imply that the combination of an α,β-α',β'-unsaturated carbonyl moiety and a vinyl-type side chain played a key role in the antibacterial activity against *Aeromonas salmonicida* AS42. The above-mentioned results indicated that these isolated steroids could be used as antibacterial agents in fish farming.

Meanwhile, compounds **2** and **6**–**10** also displayed potent inhibitory effects against the vancomycin-resistant *Enterococcus faecium* bacterium G7 with IC_{90} values ranging from 4.4 to 18.3 μM (Table 3). Among them, steroid **10** also displayed antibacterial effects against the vancomycin-resistant *Enterococcus faecium* bacteria G1, G4, and G8 with IC_{90} values of 8.0, 4.0, and 8.0 μM, respectively. The preliminary analysis of the structure-activity relationship for compounds **6**–**10** revealed that the higher degrees of unsaturation of ring A

in the steroids could keep efficacy against more individuals of the vancomycin-resistant *Enterococcus faecium* bacteria. The above-mentioned results implied that these isolates could be developed as new chemotypes of antibacterial leads against drug-resistant bacteria.

Table 3. The IC_{90} values (μM) of antibacterial bioassays of compounds **1**–**10** [a].

	1	**2**	**3**	**4**	**5**	**6**	**7**	**8**	**9**	**10**	**TC**	**OT**	**LF**
Streptococcus parauberis FP KSP28	0.3	0.5	2.7	0.1	4.9	1.1	0.5	8.9	4.4	1.0	6.3	3.1	3.1
Phoyobacterium damselae FP2244	9.1	4.2	11.0	8.5	9.8	9.2	2.2	2.2	4.4	2.0	0.1	0.1	0.1
Streptococcus parauberis SPOF3K	9.1	4.2	11.0	8.5	9.8	4.6	2.2	2.2	4.4	2.0	>50.0	25.0	3.1
Aeromonas salmonicida AS42	- [b]	-	-	-	-	-	8.8	-	-	-	12.7	0.8	0.8
Enterococcus faecium G1	-	-	-	-	-	-	8.8	-	-	8.0	0.2	0.4	>100.0
Enterococcus faecium G4	-	-	-	-	-	-	-	-	-	4.0	0.4	0.4	>100.0
Enterococcus faecium G7	-	16.8	-	-	-	18.3	8.8	8.9	4.4	8.0	0.2	0.2	>100.0
Enterococcus faecium G8	-	-	-	-	-	-	-	-	-	8.0	0.2	0.1	>100.0
Streptococcus agalactiae WR10	18.1	8.4	22.0	17.0	-	-	4.4	4.4	-	4.0	1.6	1.6	6.3

[a] Tetracycline hydrochloride (TC), oxytetracycline hydrochloride (OT), levofloxacin hydrochloride (LF) were used as positive controls. [b] '-' indicated they were not subjected to the antibacterial rescreening experiments since their inhibition rates against these bacteria were <90% in the preliminary antibacterial bioassays.

Moreover, all the isolated steroids except **5**, **6**, and **9** showed strong inhibitory activities against *Streptococcus agalactiae* WR10 with IC_{90} values ranging from 4.0 to 22.0 μM (Table 3). However, in the neuroprotective bioassays, none of these steroids displayed significant neuroprotective effects against the corticosterone-induced cellular injuries in human neuroblastoma SH-SY5Y cells at the concentration of 10 μM. In the evaluations of the anti-inflammatory effect in lipopolysaccharide (LPS)-stimulated BV-2 microglial cells, all the isolates were judged as inactive at 10 μM, neither.

3. Materials and Methods

3.1. General Experimental Procedures

Optical rotations were measured on a Perkin–Elmer 241 MC polarimeter. The X-ray measurement was made on a Bruker D8 Venture X-ray diffractometer with Cu Kα radiation (Bruker Biospin AG, Fällanden, Germany). IR spectra were recorded on a Nicolet 6700 spectrometer (Thermo Scientific, Waltham, MA, USA). NMR spectra were measured in $CDCl_3$ with a Bruker DRX-400, Bruker DRX-600, or Bruker DRX-800 spectrometer (Bruker Biospin AG, Fällanden, Germany) with the residual $CDCl_3$ (δ_H 7.26 ppm, δ_C 77.16 ppm). Chemical shifts (δ) were reported in ppm with reference to the solvent signals, and coupling constants (J) were expressed in Hz. Structural assignments were supported by ^{1}H–^{1}H COSY, HSQC, HMBC, and NOESY experiments. HREIMS data were recorded on a Finnigan-MAT-95 mass spectrometer (Finnigan-MAT, San Jose, CA, USA). HRESIMS spectra were recorded on an Agilent G6520 Q-TOF mass spectrometer. Commercial silica gel (Qingdao Haiyang Chemical Group Co., Ltd., Qingdao, China, 200–300 and 300–400 mesh) and Sephadex LH-20 gel (Amersham Biosciences, Little Chalfont, UK) were used for column chromatography (CC), and precoated-silica-gel-plates (G60 F-254, Yan Tai Zi Fu Chemical Group Co., Yantai, China) were used for analytical TLC. Reversed-phase (RP) HPLC was performed on an Agilent 1260 series liquid chromatography equipped with a DAD G1315D detector at 210 and 254 nm. A semi-preparative ODS-HG-5 column (5 μm, 250 × 9.4 mm)

was employed for the purifications. All solvents used for CC and HPLC were of analytical grade (Shanghai Chemical Reagents Co., Ltd., Shanghai, China) and chromatographic grade (Dikma Technologies Inc., Beijing, China), respectively.

3.2. Animal Material

The soft coral *Lobophytum* sp. was collected in October 2021 in Xuwen Country, Guangdong Province, China. This specimen was identified by Prof. X.-B. Li from Hainan University. A voucher specimen (No. S-21-XW-6553) is available for inspection at the Shanghai Institute of Materia Medica, Chinese Academy of Sciences.

3.3. Extraction and Isolation

The frozen animals (1275 g, dry weight) were cut into pieces and extracted exhaustively with acetone at room temperature (4 × 3.0 L, 15 min in ultrasonic bath). The organic extract was evaporated to give a brown residue, which was then partitioned between Et_2O and H_2O. The Et_2O solution was concentrated under reduced pressure to give a dark brown residue (13.4 g), which was fractionated by gradient Si gel (200–300 mesh) column chromatography (CC) (Et_2O/petroleum ether (PE), 0→100%), yielding eight fractions (A–H). Fraction C was chromatographed over Sephadex LH-20 CC (PE/CH_2Cl_2/MeOH, 2:1:1) to give compound **10** (1.5 mg) and a mixture. This mixture was further purified through a silica gel CC (300–400 mesh, PE:Et_2O, 12:1) followed by RP-HPLC (80% MeOH, 0.8 mL/min) to afford compound **6** (3.8 mg, t_R = 31.3 min). Fraction D was subjected to a column of Sephadex LH-20 eluted with PE/CH_2Cl_2/MeOH (2:1:1) to yield three subfractions (D1–D3). Compound **8** (1.5 mg, t_R = 20.0 min) was obtained from the D1 through a silica gel CC (300–400 mesh, PE:Et_2O, 10:1) followed by RP-HPLC (85% CH_3CN, 1.0 mL/min). Compound **9** (2.0 mg, t_R = 29.1 min) was isolated from the D2 through silica gel CC (300–400 mesh, PE:Et_2O, 10:1) followed by RP-HPLC (85% CH_3CN, 1.0 mL/min). Compounds **4** (1.7 mg, t_R = 25.9 min) and **5** (0.8 mg, t_R = 22.0 min) were obtained from the D3 through silica gel CC (300–400 mesh, PE:Et_2O, 10:1) followed by RP-HPLC (77% CH_3CN, 1.0 mL/min). Fraction E was subjected to Sephadex LH-20 CC (PE/CH_2Cl_2/MeOH, 2:1:1), followed by RP-HPLC (75% CH_3CN, 0.6 mL/min) to give compound **7** (3.1 mg, t_R = 25.8 min). Fraction F was subjected to a column of Sephadex LH-20 eluted with PE/CH_2Cl_2/MeOH (2:1:1) and further divided into two subfractions, F1 and F2, by the following silica gel CC (300–400 mesh, PE:Et_2O, 3:1). Compounds **1** (2.6 mg, t_R = 8.7 min) and **3** (1.1 mg, t_R = 12.6 min) were obtained from F2 by RP-HPLC (65% CH_3CN, 0.8 mL/min) while **2** (1.6 mg, t_R = 28.0 min) was obtained from F1 by RP-HPLC (75% CH_3CN, 0.8 mL/min).

3.4. Spectroscopic Data of Compounds

Lobosteroid A (**1**): Colorless crystal; $[\alpha]_{20}^{D}$ −3.8 (c 0.26, $CHCl_3$); IR (KBr): ν_{max} 3358, 2922, 2851, 1661, 1632, 1468, 1180 cm^{-1}; ^1H and ^{13}C NMR ($CDCl_3$, 800 and 125 MHz; see Tables 1 and 2); HRESIMS *m*/*z* 427.3210 $[M + H]^+$ (calcd. for $C_{28}H_{43}O_3$, 427.3207).

Lobosteroid B (**2**): White amorphous powder; $[\alpha]_{20}^{D}$ +14.0 (c 0.16, $CHCl_3$); IR (KBr): ν_{max} 3358, 2925, 2852, 1664, 1631, 1467, 887 cm^{-1}; ^1H and ^{13}C NMR ($CDCl_3$, 600 and 150 MHz; see Tables 1 and 2); HRESIMS *m*/*z* 411.3255 $[M + H]^+$ (calcd. for $C_{28}H_{43}O_2$, 411.3258).

Lobosteroid C (**3**): White amorphous powder; $[\alpha]_{20}^{D}$ +18.2 (c 0.05, CH_3OH); IR (KBr): ν_{max} 3359, 2923, 2852, 1742, 1662, 1468, 1236 cm^{-1}; ^1H and ^{13}C NMR ($CDCl_3$, 600 and 150 MHz; see Tables 1 and 2); HRESIMS *m*/*z* 469.3318 $[M + H]^+$ (calcd. for $C_{30}H_{45}O_4$, 469.3312).

Lobosteroid D (**4**): White amorphous powder; $[\alpha]_{20}^{D}$ +9.2 (c 0.17, $CHCl_3$); IR (KBr): ν_{max} 3359, 2923, 2852, 1660, 1633, 1468 cm^{-1}; ^1H and ^{13}C NMR (CDCl3, 600 and 200 MHz; see Tables 1 and 2); HRESIMS *m*/*z* 443.3520 $[M + H]^+$ (calcd. for $C_{29}H_{47}O_3$, 443.3520).

Lobosteroid E (**5**): White amorphous powder; $[\alpha]_{20}^{D}$ +11.9 (c 0.08, $CHCl_3$); IR (KBr): ν_{max} 3358, 2922, 2851, 1660, 1633, 1468 cm^{-1}; ^1H and ^{13}C NMR (CDCl3, 600 and 200 MHz; see Tables 1 and 2); HRESIMS *m*/*z* 413.3411 $[M + H]^+$ (calcd. for $C_{28}H_{45}O_2$, 413.3414).

Lobosteroid F (**6**): White amorphous powder; $[\alpha]_{20}^{D}$ −7.9 (c 0.38, $CHCl_3$); IR (KBr): ν_{max} 3300, 2949, 2869, 1455, 1377, 1044 cm^{-1}; ^1H and ^{13}C NMR ($CDCl_3$, 400 and 150 MHz; see Tables 1 and 2); HREIMS *m*/*z* 424.3325 $[M - H_2O]^+$ (calcd. for $C_{29}H_{44}O_2$, 424.3336).

3.5. X-ray Crystallographic Analysis for Compound **1**

Lobosteroid A (**1**) was crystallized from MeOH at room temperature. $C_{28}H_{43}O_3$, Mr = 426.61, monoclinic, crystal size 0.12 × 0.08 × 0.05 mm^3, space group $P2_12_12_1$, a = 11.7623(13) Å, b = 11.875(2) Å, c = 17.1256(15) Å, V = 2392.0(6) $Å^3$, Z = 4, ρ_{calcd} = 1.185 g/cm^3, F(000) = 936.0, 31,225 collected reflections, 4920 independent reflections (R_{int} = 0.0522, R_{sigma} = 0.0310), final R1 = 0.0353 (wR_2 = 0.0904) reflections with $I \geq 2\sigma$ (I), R_1 = 0.0383, wR_2 = 0.0951 for all unique data. The X-ray measurements were made on a Bruker D8 Venture X-ray diffractometer with Cu Kα radiation (λ = 1.54178 Å) at 170.0 K. The collected data integration and reduction were processed with SAINT V8.37A software, and multiscan absorption corrections were performed using the SADABS program. The structure was solved with the SHELXT [39] structure solution program using intrinsic phasing and refined with the SHELXL [40] refinement package using least squares minimization. Crystallographic data for **1** were deposited at the Cambridge Crystallographic Data Centre (Deposition nos. CCDC 2282723). Copies of these data can be obtained free of charge via www.ccdc.cam.ac.uk (accessed on 19 July 2023), or from the Cambridge Crystallographic Data Centre, 12 Union Road, Cambridge CB21EZ, UK. [Fax: (+44) 1223-336-033. E-mail: deposit@ccdc.cam.ac.uk.]

3.6. Antibacterial Bioassays

The marine strains *Streptococcus parauberis* FP KSP28, *Streptococcus parauberis* SPOF3K, *Phoyoba cteriumdamselae* FP2244, and *Aeromonas salmonicida* AS42 were provided by National Fisheries Research & Development Institute, Korea. The strain *Streptococcus agalactiae* WR10 was provided by the Chinese Academy of Tropical Agricultural Sciences. The vancomycin-resistant *Enterococcus faecium* bacteria G1, G4, G7, and G8 were provided by Ruijin Hospital, Shanghai Jiao Tong University School of Medicine. The minimum inhibitory concentration for 90% (MIC_{90}) values for all antimicrobial agents was measured by the 96-well microdilution method. Mueller–Hinton II broth (cation-adjusted, BD 212322) was used for MIC_{90} value determination. Generally, compounds were dissolved with DMSO to 20 mM as stock solutions. All samples were diluted with culture broth to 500 μM as the initial concentration. Further, 1:2 serial dilutions were performed by the addition of culture broth to reach concentrations ranging from 500 μM to 0.24 μM. 100 μL of each dilution was distributed in 96-well plates, as well as sterile controls, growth controls (containing culture broth plus DMSO, without compounds), and positive controls (containing culture broth plus control antibiotics such as tetracycline). Each test and growth control well was inoculated with 5 μL of an exponential-phase bacterial suspension (about 10^5 CFU/well). The 96-well plates were incubated at 37 °C for 24 h. MIC_{90} values of these compounds were defined as the lowest concentration to inhibit bacterial growth completely. All MIC_{90} values were interpreted according to the recommendations of the Clinical and Laboratory Standards Institute (CLSI). Tetracycline hydrochloride (TC), oxytetracycline hydrochloride (OT), and levofloxacin hydrochloride (LF) were used as positive controls (Table 3).

4. Conclusions

In summary, six new steroids, lobosteroids A–F (**1**–**6**), together with four known compounds **7**–**10**, were isolated from the Chinese soft coral *Lobophytum* sp. The chemical diversity of new steroids was mainly attributed to the high oxidation, which was characterized by the conjugated enone or dienone system of the nucleus and diverse oxidation of side chains. Although many steroids were reported from soft corals, those with an α,β-α',β'-unsaturated carbonyl or an α,β-unsaturated carbonyl moiety in ring A, or the existence of a 5α,8α-epidioxy system in ring B were rarely found from the genus *Lobophytum*. The discovery of steroids **1**–**6** expanded the diverse and complex array of steroids, which

is still a research hotspot of marine natural products. In the bioassays, all of the isolates displayed significant antibacterial activities against the fish pathogenic bacteria *Streptococcus parauberis* FP KSP28, *Phoyobacterium damselae* FP2244, and *Streptococcus parauberis* SPOF3K with IC_{90} values ranging from 0.1 to 11.0 μM. Meanwhile, compounds **2** and **6**–**10** exhibited excellent antibacterial activities against the vancomycin-resistant *Enterococcus faecium* bacterium G7 with IC_{90} values ranging from 4.4 to 18.3 μM. These new findings implied that these isolated steroids could be developed as new chemotypes of antibacterial leads.

Supplementary Materials: The following supporting information can be downloaded at: https://www.mdpi.com/article/10.3390/md21080457/s1, Figures S1–S48: NMR, HRESIMS, HREIMS, and IR data of compounds **1**–**6**.

Author Contributions: Conceptualization, L.-F.L., H.W. and Y.-W.G.; methodology, M.-Z.S., L.-F.L., H.W. and Y.-W.G.; validation, Z.-Y.X., M.-M.S. and M.-Z.S.; formal analysis, Z.-Y.X. and M.-M.S.; investigation, Z.-Y.X., Y.J. and M.-M.S.; resources, L.-G.Y.; data curation, Z.-Y.X. and M.-M.S.; writing—original draft preparation, Z.-Y.X.; writing—review and editing, L.-F.L. and Y.-W.G.; supervision, H.W. and Y.-W.G.; project administration, Y.-W.G.; funding acquisition, L.-F.L., H.W. and Y.-W.G. All authors have read and agreed to the published version of the manuscript.

Funding: This work was financially supported by the National Key Research and Development Program of China (No. 2022YFC2804100) and the National Natural Science Foundation of China (No. 81991521, 41876194).

Institutional Review Board Statement: Not applicable.

Data Availability Statement: Data are contained within the article or Supplementary Materials.

Acknowledgments: We appreciate the grants from the Shandong Laboratory of Yantai Drug Discovery, Bohai Rim Advanced Research Institute for Drug Discovery, and thank X.-B. Li from Hainan University for the taxonomic identification of the soft coral material.

Conflicts of Interest: The authors declare no conflict of interest.

References

1. Carroll, A.R.; Copp, B.R.; Davis, R.A.; Keyzers, R.A.; Prinsep, M.R. Marine natural products. *Nat. Prod. Rep.* **2023**, *40*, 275–325. [CrossRef]
2. Savić, M.P.; Sakač, M.N.; Kuzminac, I.Z.; Ajduković, J.J. Structural diversity of bioactive steroid compounds isolated from soft corals in the period 2015–2020. *J. Steroid Biochem.* **2022**, *218*, 106061. [CrossRef] [PubMed]
3. Shao, Z.-Y.; Zhu, D.-Y.; Guo, Y.-W. Nanjiols A−C, new steroids from the Chinese soft coral *Nephthea bayeri*. *J. Nat. Prod.* **2002**, *65*, 1675–1677. [CrossRef] [PubMed]
4. Liang, L.-F.; Wang, X.-J.; Zhang, H.-Y.; Liu, H.-L.; Li, J.; Lan, L.-F.; Zhang, W.; Guo, Y.-W. Bioactive polyhydroxylated steroids from the Hainan soft coral *Sinularia depressa* Tixier-Durivault. *Bioorg. Med. Chem. Lett.* **2013**, *23*, 1334–1337. [CrossRef]
5. Yan, X.-H.; Liu, H.-L.; Guo, Y.-W. Ximaosteroids A–D, new steroids from the Hainan soft coral *Scleronephthya* sp. *Steroids* **2009**, *74*, 1061–1065. [CrossRef] [PubMed]
6. Chen, W.-T.; Liu, H.-L.; Yao, L.-G.; Guo, Y.-W. 9,11-Secosteroids and polyhydroxylated steroids from two South China Sea soft corals *Sarcophyton trocheliophorum* and *Sinularia flexibilis*. *Steroids* **2014**, *92*, 56–61. [CrossRef] [PubMed]
7. Liu, J.; Wu, X.; Yang, M.; Gu, Y.-C.; Yao, L.-G.; Huan, X.-J.; Miao, Z.-H.; Luo, H.; Guo, Y.-W. Erectsterates A and B, a pair of novel highly degraded steroid derivatives from the South China Sea soft coral *Sinularia erecta*. *Steroids* **2020**, *161*, 108681. [CrossRef] [PubMed]
8. Xu, T.; Zhao, Q.-M.; Yao, L.-G.; Lan, L.-F.; Li, S.-W.; Guo, Y.-W. Sinulasterols D–G, four new antibacterial steroids from the South China sea soft coral *Sinularia depressa*. *Steroids* **2023**, *192*, 109182. [CrossRef]
9. Li, S.-W.; Liu, J.; Fu, Y.; Yao, L.-G.; Zhang, H.-Y.; Wang, H.; Guo, Y.-W. Anti-inflammatory steroids from the South China Sea soft coral *Lobophytum sarcophytoides*. *Chem. Biodivers.* **2023**, *20*, e202300821. [CrossRef] [PubMed]
10. Zhang, Q.; Liang, L.-F.; Miao, Z.-H.; Wu, B.; Guo, Y.-W. Cytotoxic polyhydroxylated steroids from the South China Sea soft coral *Lobophytum* sp. *Steroids* **2019**, *141*, 76–80. [CrossRef]
11. Yang, M.; Liang, L.-F.; Li, H.; Tang, W.; Guo, Y.-W. A new 5α,8α-epidioxysterol with immunosuppressive activity from the South China Sea soft coral *Sinularia* sp. *Nat. Prod. Res.* **2020**, *34*, 1814–1819. [CrossRef]
12. Ermolenko, E.V.; Imbs, A.B.; Gloriozova, T.A.; Poroikov, V.V.; Sikorskaya, T.V.; Dembitsky, V.M. Chemical diversity of soft coral steroids and their pharmacological activities. *Mar. Drugs* **2020**, *18*, 613. [CrossRef]

13. Rodrigues, I.G.; Miguel, M.G.; Mnif, W. A brief review on new naturally occurring cembranoid diterpene derivatives from the soft corals of the genera *Sarcophyton*, *Sinularia*, and *Lobophytum* since 2016. *Molecules* **2019**, *24*, 781. [CrossRef]
14. Li, S.-W.; Cuadrado, C.; Yao, L.-G.; Daranas, A.H.; Guo, Y.-W. Quantum mechanical–NMR-aided configuration and conformation of two unreported macrocycles isolated from the soft coral *Lobophytum* sp.: Energy calculations versus coupling constants. *Org. Lett.* **2020**, *22*, 4093–4096. [CrossRef]
15. Zhang, D.; Wang, Z.; Han, X.; Li, X.-L.; Lu, Z.-Y.; Dou, B.-B.; Zhang, W.-Z.; Tang, X.-L.; Li, P.-L.; Li, G.-Q. Four bioactive new steroids from the soft coral *Lobophytum pauciflorum* collected in South China Sea. *Beilstein J. Org. Chem.* **2022**, *18*, 374–380. [CrossRef]
16. Ohno, O.; Mizuno, E.; Miyamoto, J.; Hoshina, T.; Sano, T.; Matsuno, K. Inhibition of lipopolysaccharide-induced inflammatory signaling by soft coral-derived prostaglandin A_2 in RAW264.7 cells. *Mar. Drugs* **2022**, *20*, 316. [CrossRef]
17. Li, Z.-Y.; Li, C.-Y.; Lai, K.-H.; Liao, M.-Y.; Wang, W.-H.; Chung, H.-M. Chemical constituents from the octocoral *Lobophytum sarcophytoides*. *Chem. Nat. Compd.* **2022**, *58*, 1167–1169. [CrossRef]
18. Peng, B.-R.; Lu, M.-C.; El-Shazly, M.; Wu, S.-L.; Lai, K.-H.; Su, J.-H. Aquaculture soft coral *Lobophytum crassum* as a producer of anti-proliferative cembranoids. *Mar. Drugs* **2018**, *16*, 15. [CrossRef]
19. Huang, C.-Y.; Tseng, W.-R.; Ahmed, F.A.; Chiang, P.-L.; Tai, C.-J.; Hwang, T.-L.; Dai, C.-F.; Sheu, J.-H. Anti-inflammatory polyoxygenated steroids from the soft coral *Lobophytum michaelae*. *Mar. Drugs* **2018**, *16*, 93. [CrossRef]
20. Rahelivao, M.P.; Lübken, T.; Gruner, M.; Kataeva, O.; Ralambondrahety, R.; Andriamanantoanina, H.; Checinski, M.P.; Bauer, I.; Knölker, H.-J. Isolation and structure elucidation of natural products of three soft corals and a sponge from the coast of Madagascar. *Org. Biomol. Chem.* **2017**, *15*, 2593–2608.
21. Aboutabl, E.A.; Selim, N.M.; Azzam, S.M.; Michel, C.G.; Hegazy, M.F.; Ali, A.M.; Hussein, A.A. Polyhydroxy sterols isolated from the Red Sea soft coral *Lobophytum crassum* and their cytotoxic activity. *Nat. Prod. Commun.* **2017**, *12*, 233–235. [CrossRef]
22. Hegazy, M.-E.F.; Mohamed, T.A.; Elshamy, A.I.; Hassanien, A.A.; Abdel-Azim, N.S.; Shreadah, M.A.; Abdelgawad, I.I.; Elkady, E.M.; Paré, P.W. A new steroid from the Red Sea soft coral *Lobophytum lobophytum*. *Nat. Prod. Res.* **2016**, *30*, 340–344. [CrossRef]
23. Chau, V.M.; Phan, V.K.; Nguyen, X.N.; Nguyen, X.C.; Nguyen, P.T.; Nguyen, H.N.; Hoang, L.T.A.; Do, C.T.; Dinh, T.T.T.; Kang, H.-K.; et al. Cytotoxic and antioxidant activities of diterpenes and sterols from the Vietnamese soft coral *Lobophytum compactum*. *Bioorg. Med. Chem. Lett.* **2011**, *21*, 2155–2159.
24. Yeffet, D.; Rudi, A.; Ketzinel, S.; Benayahu, Y.; Kashman, Y. Auroside, a xylosyl-sterol, and patusterol A and B, two hydroxylated sterols, from two soft corals *Eleutherobia aurea* and *Lobophytum patulum*. *Nat. Prod. Commun.* **2010**, *5*, 205–210. [CrossRef] [PubMed]
25. Ye, F.; Zhou, Y.-B.; Li, J.; Gu, Y.-C.; Guo, Y.-W.; Li, X.-W. New steroids from the South China Sea soft coral *Lobophytum* sp. *Chem. Biodivers.* **2020**, *17*, e2000214. [CrossRef] [PubMed]
26. Radhika, P.; Asolkar, R.N.; Laatsch, H. An acetoxygenated analogue of ergosterol from a soft coral of the genus Lobophytum. *Nat. Prod. Res.* **2004**, *18*, 575–579. [CrossRef] [PubMed]
27. Morris, L.A.; Christie, E.M.; Jaspars, M.; van Ofwegen, L.P. A bioactive secosterol with an unusual A- and B-ring oxygenation pattern isolated from an Indonesian soft coral *Lobophytum* sp. *J. Nat. Prod.* **1998**, *61*, 538–541. [CrossRef]
28. Radhika, P.; Cabeza, M.; Bratoeff, E.; García, G. 5α-Reductase inhibition activity of steroids isolated from marine soft corals. *Steroids* **2004**, *69*, 439–444.
29. Liu, J.; Gu, Y.-C.; Su, M.-Z.; Guo, Y.-W. Chemistry and bioactivity of secondary metabolites from South China Sea marine fauna and flora: Recent research advances and perspective. *Acta Pharmacol. Sin.* **2022**, *43*, 3062–3079. [PubMed]
30. Song, Y.-T.; Yu, D.-D.; Su, M.Z.; Luo, H.; Cao, J.-G.; Yao, L.-G.; Liang, L.-F.; Guo, Y.-W.; Yang, F. Anti-tumor cembrane diterpenoids from the South China Sea soft coral *Lobophytum* sp. *Chem. Biodivers.* **2023**, *20*, e202300217. [CrossRef]
31. Díaz-Marrero, A.R.; Porras, G.; Aragón, Z.; de la Rosa, J.M.; Dorta, E.; Cueto, M.; D'Croz, L.; Maté, J.; Darias, J. Carijodienone from the octocoral *Carijoa multiflora*. A spiropregnane-based steroid. *J. Nat. Prod.* **2011**, *74*, 292–295. [PubMed]
32. Seo, Y.; Jung, J.H.; Rho, J.-R.; Shin, J.; Song, J.-I. Isolation of novel bioactive steroids from the soft coral *Alcyonium gracillimum*. *Tetrahedron* **1995**, *51*, 2497–2506.
33. Wu, S.-L.; Wang, G.-H.; Dai, C.-F.; Sheu, J.-H. Pregnane-based steroids from a Formosan gorgonian *Subergorgia mollis*. *J. Chin. Chem. Soc.* **2004**, *51*, 205–208.
34. Blackman, A.J.; Heaton, A.; Skelton, B.W.; White, A.H. Pregnane derivatives from two soft corals of the genus *Capnella*. *Aust. J. Chem.* **1985**, *38*, 565–573. [CrossRef]
35. Yan, X.-H.; Liu, H.-L.; Huang, H.; Li, X.-B.; Guo, Y.-W. Steroids with aromatic A-rings from the Hainan soft coral *Dendronephthya studeri* Ridley. *J. Nat. Prod.* **2010**, *74*, 175–180. [PubMed]
36. Marinozzi, M.; Castro Navas, F.F.; Maggioni, D.; Carosati, E.; Bocci, G.; Carloncelli, M.; Giorgi, G.; Cruciani, G.; Fontana, R.; Russo, V. Side-chain modified ergosterol and stigmasterol derivatives as liver X receptor agonists. *J. Med. Chem.* **2017**, *60*, 6548–6562. [PubMed]
37. Yan, X.-H.; Lin, L.-P.; Ding, J.; Guo, Y.-W. Methyl spongoate, a cytotoxic steroid from the Sanya soft coral *Spongodes* sp. *Bioorg. Med. Chem. Lett.* **2007**, *17*, 2661–2663. [CrossRef] [PubMed]
38. Ahmed, A.F.; Wu, M.-H.; Wu, Y.-C.; Dai, C.-F.; Sheu, J.-H. Metabolites with cytotoxic activity from the Formosan soft coral *Cladiella australis*. *J. Chin. Chem. Soc.* **2006**, *53*, 489–494. [CrossRef]

39. Sheldrick, G.M. *SHELXT*—Integrated space-group and crystal-structure determination. *Acta Crystallogr.* **2015**, *A71*, 3–8.
40. Sheldrick, G.M. Crystal structure refinement with *SHELXL*. *Acta Crystallogr.* **2015**, *C71*, 3–8.